

RETARDATION EFFECTS IN $ed \rightarrow e'np$ REACTION

V.V.Burov, A.A.Goy*, S.Eh.Sus'kov*

Electrodisintegration of the deuteron near pion threshold with allowance for retardation effects in meson exchange currents is studied. It is shown that retardation effects should be taken into account at large transfer momenta ($t > 10 \text{ fm}^{-2}$). The radial dependence of the matrix elements for $d \rightarrow {}^1S_0$ -transition has been investigated. It is found that the inclusion of meson exchange currents with allowance for retardation effects is important at $r = 1-1.5 \text{ fm}$, when $t < 30 \text{ fm}^{-2}$.

The investigation has been performed at the Laboratory of Theoretical Physics, JINR.

Эффекты запаздывания в $ed \rightarrow e'np$ -реакции

В.В.Буров, А.А.Гой, С.Э.Суськов

Исследован электроразвал дейтрона на пороге пинообразования с учетом эффектов запаздывания в мезонных обменных токах. Показана необходимость учета эффектов запаздывания в области больших импульсов передачи ($t > 10 \text{ фм}^{-2}$). Рассмотрена радиальная зависимость матричных элементов для $d \rightarrow {}^1S_0$ -перехода. Установлено, что вклад мезонных обменных токов с учетом эффектов запаздывания наиболее существенен при $r = 1-1.5 \text{ фм}$ для $t < 30 \text{ фм}^{-2}$.

Работа выполнена в Лаборатории теоретической физики ОИЯИ.

1. Introduction

Magnetic $M1$ -transition in the $ed \rightarrow e'np$ reaction with inclusion of meson exchange currents has been studied earlier in refs. [1—7]. Detailed calculations have been made with allowance for seagull and meson currents (fig.1 (a), (b)). However, the investigations of the retardation effects have not been done yet. The reason is the lack of experimental results at large momentum transfer. In this case the traditional set of meson exchange currents (see fig. 1) was quite enough to get the correct information on the differential cross section in a small region of transfer momenta.

*Far-East State University, Vladivostok, Russia

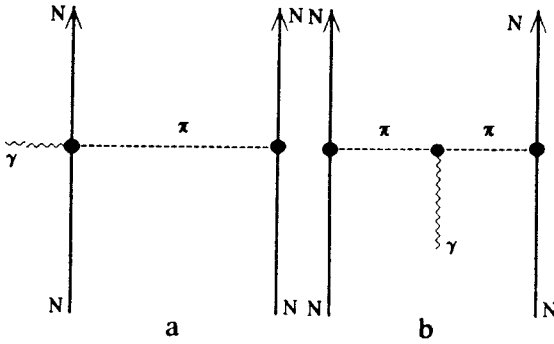


Fig.1. Diagrams of seagull (a) and meson (b) currents

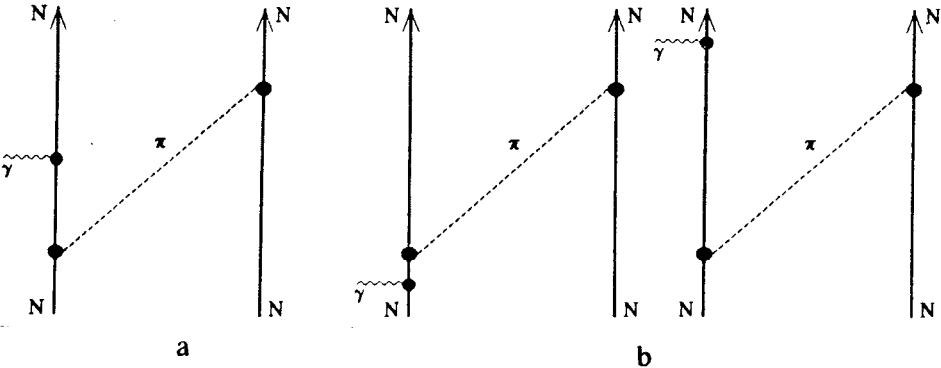


Fig.2. Diagrams of recoil (a) renormalization (b) currents

At present the available experimental data on the differential cross section are known up to about 1 GeV that allow one to investigate the electrodisintegration near threshold at short distances where the relativistic contributions have to be important.

The retardation of meson exchange currents is one of significant relativistic effects, whose investigation has been done. In ref. [8] the retardation current was studied for the elastic $e-d$ scattering. It was shown that the inclusion of retardation meson exchange current into the structure function $B(q^2)$ has a considerable effect at large transfer momenta. Moreover, for the structure function $A(q^2)$ the contribution of retardation effects worsens the agreement with experimental data thus compelling one to take account of other effects, for instance, quark degrees of freedom. That situation provokes the investigation of the deuteron structure when all the contributions of meson exchange currents are taken into account including retardation effects.

In the present paper, the electrodisintegration of the deuteron with allowance for retardation effect has been investigated.

Moreover, the radial dependence of the matrix elements for $d \rightarrow {}^1S_0$ transition with allowance for retardation effect has been studied. It was founded earlier in ref. [7] that the meson exchange currents (fig.1) dominate

if the relative distance between two nucleons is between 1 and 1.4 fm for $t \leq 30 \text{ fm}^{-2}$. In our work the influence of retardation effects is studied, which is necessary to get a realistic picture of the radial dependence at high momentum transfers.

2. Model

According to ref. [6] the differential cross section for the $d \rightarrow {}^1S_0$ -transition has the form

$$\begin{aligned} \frac{d^2\sigma}{d\Omega d\omega} = & \frac{16}{3} \alpha^2 \frac{k_f^2}{q^2} \frac{KM}{t^2} \sin^2 \frac{1}{2} \theta ((k_i + k_f)^2 - \\ & - 2k_i k_f \cos^2 \frac{1}{2} \theta) |\langle {}^1S_0 || T_1^{\text{Mag}} || d \rangle|^2, \end{aligned} \quad (1)$$

$k_{i(f)}$ is the initial (final) momentum of the electron, q is the vector of momentum transfer, t stands for the four momentum transfer. The magnetic multipole T_1^{Mag} is expressed through the isovector current operator J as follows

$$T_1^{\text{Mag}}(q) = \int j_1(qx) Y_{111}^M(\Omega_x) J dx. \quad (2)$$

The expression for the isovector retardation current is derived in the framework of the S -matrix method for $M1$ - transition due to π exchange. We have the following equation:

$$J^R = J^A + J^B \quad (3)$$

with

$$\begin{aligned} J^A = & -iG_M^\nu(t) \frac{f^2}{32\pi M^2 m_\pi^2} \frac{1}{\omega^4} \left(i(\tau_1 \times \tau_2)_3 + \tau_3^2 \right) \times \\ & \times (\sigma_1 \cdot k_2) (\sigma_1 \times q) (q \cdot k_2) (\sigma_2 \cdot k_2), \end{aligned} \quad (4)$$

$$J^B = -F_1^\nu(t) \frac{f^2}{32\pi M^2 m_\pi^2} \frac{1}{\omega^4} \left(i(\tau_1 \times \tau_2)_3 + \tau_3^2 \right) k_2 (\sigma_1 \cdot k_2) (q \cdot k_2) (\sigma_2 \cdot k_2). \quad (5)$$

Here $f^2/4\pi = 0.08$, M is the nucleon mass, m_π denotes the pion mass, $k_{1(2)} = p'_{1,2} - p_{1,2}$ ($p_{1,2}$, $p'_{1,2}$ are the initial and final momenta of two nucleons), ω is the pion energy,

$$G_M^y(t) = \frac{4.706}{1 + \frac{t}{18.23 \text{ fm}^{-2}}}, \quad (6)$$

$$F_1^y(t) = \frac{1}{\left(1 + \frac{t}{18.23 \text{ fm}^{-2}}\right)^2} \frac{1}{1 + \frac{t}{4M^2}} \left(1 + 4.706 \frac{t}{4M^2}\right) \quad (7)$$

(see [6]). The matrix elements for seagull and meson currents have been derived in ref. [6]. In this paper we have determined the matrix element for the retardation current. The retardation matrix element for $d \rightarrow {}^1S_0$ -transition has the following form

$$\langle {}^1S_0 || T_{1,R}^{\text{Mag}} || d \rangle = i \frac{q}{\sqrt{2\pi}} \int_0^\infty \eta(r, t) dt. \quad (8)$$

Here

$$\begin{aligned} \eta(r, t) = & G_M^y(t) \frac{f^2}{80\pi^3 M^2 m_\pi^2} u_0(r) (j_1(\frac{1}{2}qr) (\frac{1}{\sqrt{2}} u(r) 19I_1(r) + \\ & + w(r) \frac{1}{10} (-13I_1(r) - 8I_3(r))) + j_3(\frac{1}{2}qr) (\frac{1}{\sqrt{2}} u(r) 11I_3(r) + \\ & + W(r) \frac{1}{10} (7I_1(r) - 28I_3(r))))), \end{aligned} \quad (9)$$

where $u(r)$, $w(r)$, $u_0(r)$ are wave functions of S , D states of the deuteron and 1S_0 -final state, respectively. The radial functions $I_l(r)$ are given by

$$I_l(r) = \int_0^\infty k^5 j_l(kr) \frac{K_\pi^2(k)}{(k^2 + m_\pi^2)^2} dk. \quad (10)$$

Kinematical quantities are related in the following way

$$q = \sqrt{\frac{((M_n + M_p + E_{np})^2 - M_d^2 + t)^2}{4M_d^2} + t}, \quad (11)$$

where M_n , M_p , M_d are the neutron, proton and deuteron mass, respectively. For $r \rightarrow \infty$, we have

$$u_0(r) \rightarrow \frac{1}{K} \sin(Kr + \delta_0). \quad (12)$$

The momentum K is related to the relative energy of np system E_{np} as follows

$$E_{np} = \frac{K^2}{M}. \quad (13)$$

Note that the result (8) is independent of J^B .

To determine the realistic properties of a two-nucleon system, the inner structure of nuclei at short distances has to be taken into account. In this case the bare πNN vertex has to be parametrized by the vertex form factor $K_\pi(k)$. We shall investigate two parametrization forms of the vertex form factor. The first one is of a monopole form. According to ref. [6] we have

$$K_\pi(k) = \frac{\Lambda_\pi^2 - m_\pi^2}{\Lambda_\pi^2 + k^2}. \quad (14)$$

The second parametrization ensures the monopole behavior at small k^2 that is usually used in the low-energy reactions, and the $(k^2)^{-3}$ decrease at large k^2 assigned by quantum chromodynamics [10] is given by

$$K_\pi(k) = \frac{1}{\left(1 + \frac{k^2}{\Lambda_{1,\pi}^2}\right) \left(1 + \frac{k^4}{\Lambda_{2,\pi}^4}\right)}. \quad (15)$$

We shall investigate different values of the cut-off parameters related to the rms of the nucleon: 0.48 fm and 0.7 fm. Here $\Lambda_\pi = 1.25$ GeV or 0.85 GeV, respectively. A detailed analysis of rms was done in ref. [6]. The cut-off parameters $\Lambda_{1,\pi} = 0.99$ GeV, $\Lambda_{2,\pi} = 2.58$ GeV were determined in ref. [10]. The calculations with the vertex form factor (15) were made with the following renormalization of the coupling constant f :

$$f = f \left(1 - \frac{m_\pi^2}{\Lambda_\pi^2} \right). \quad (16)$$

3. Results and Discussion

Calculations of the differential cross section have been done with the relative energy of np system $E_{np} = 1.5$ MeV and scattering angle $\theta = 155^\circ$ with the use of wave functions of the Paris potential. The results for the differential cross section with allowance for meson exchange currents (figs.1,2) are shown in fig.3.

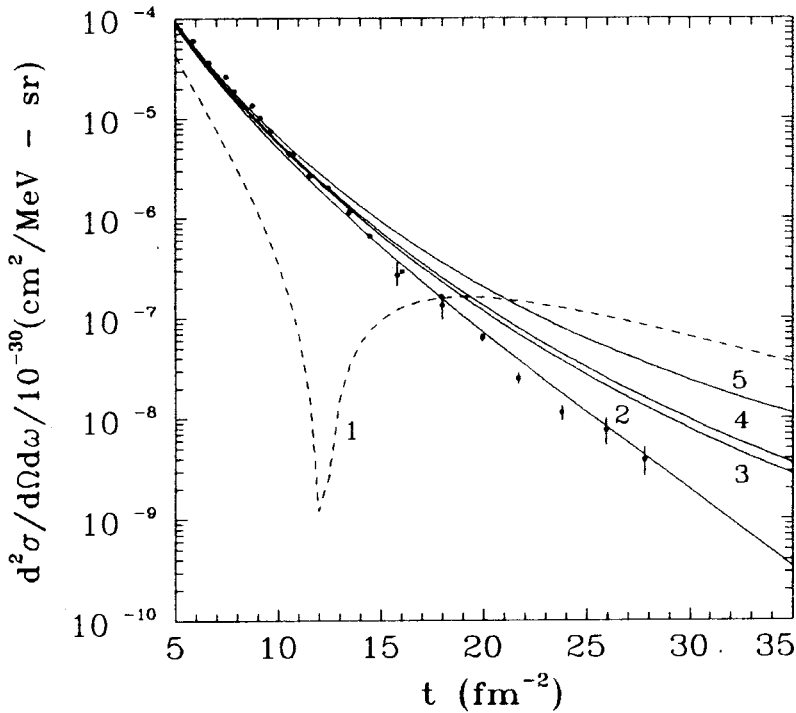


Fig.3. Differential cross section. The dashed line 1 is the impulse approximation, 2 is the calculation with the vertex form factor (14), and $\Lambda_\pi = 0.85$ GeV, 3,4 are the calculations with the vertex form factor (15), $\Lambda_\pi = 0.85$ GeV and $\Lambda_\pi = 1.25$ GeV, respectively, 5 is the calculation with the vertex form factor (14) and $\Lambda_\pi = 1.25$ GeV. The experimental data from [11], [12]

It is seen that the results are very sensitive to the parametrization form of the vertex form factor and cut-off parameters. First of all we note that the calculation with monopole parametrization form (14) and cut-off parameter $\Lambda_\pi = 1.25$ GeV (curve 5) destroys the agreement with experimental results in the region of $t > 10 \text{ fm}^{-2}$.

The inclusion of $\Lambda_\pi = 0.85$ GeV, curve 2, leads to a more positive result which is not in contradiction with the experimental data.

Curves 3,4 (see (16)) show the calculations of the same differential cross section but with the rapid-decreasing vertex form factor (15). Here, in contrast with the monopole vertex form factor, we get results in contradiction with the experimental data in the region of $t > 13 \text{ fm}^{-2}$.

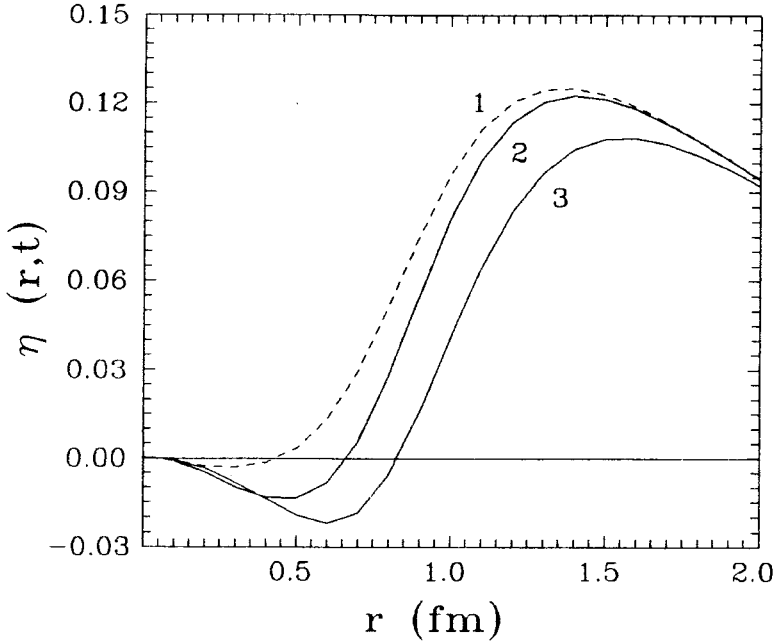


Fig.4. The dashed line 1 is the calculation for point particles. 2 is the inclusion of MEC with allowance for retardation effects (S+M+R) and $\Lambda_\pi = 1.25$ GeV. 3 is the inclusion of MEC with allowance for retardation effects (S+M+R), with $\Lambda_\pi = 0.85$ GeV. The calculations were made with the vertex form factor (14) and $t = 0 \text{ fm}^{-2}$

Now let us consider the radial dependence of the matrix elements on the momentum t . Figures 4,5 show the calculations of the radial functions $\eta(r, t)$ for the vertex form factor (14) with $\Lambda_\pi = 1.25$ GeV and $\Lambda_\pi = 0.85$ GeV for momenta transfer $t = 0 \text{ fm}^{-2}$ and $t = 30 \text{ fm}^{-2}$.

It is seen that if $t = 0 \text{ fm}^{-2}$, the retardation effects are absent (fig.4 curve 2,3). In this case curves 2 and 3 are absolutely identical with the calculation without retardation current. The total result dominates in the range of relative distances of about 1.4 fm for $\Lambda_\pi = 1.25$ GeV and 1.5 fm for $\Lambda_\pi = 0.85$ GeV.

However, the retardation effects are more manifest in the calculations at large transfer momenta.

Comparing the result obtained with allowance for retardation effects, fig.5 (curves 3,5), with the analogous calculation with the use of the seagull

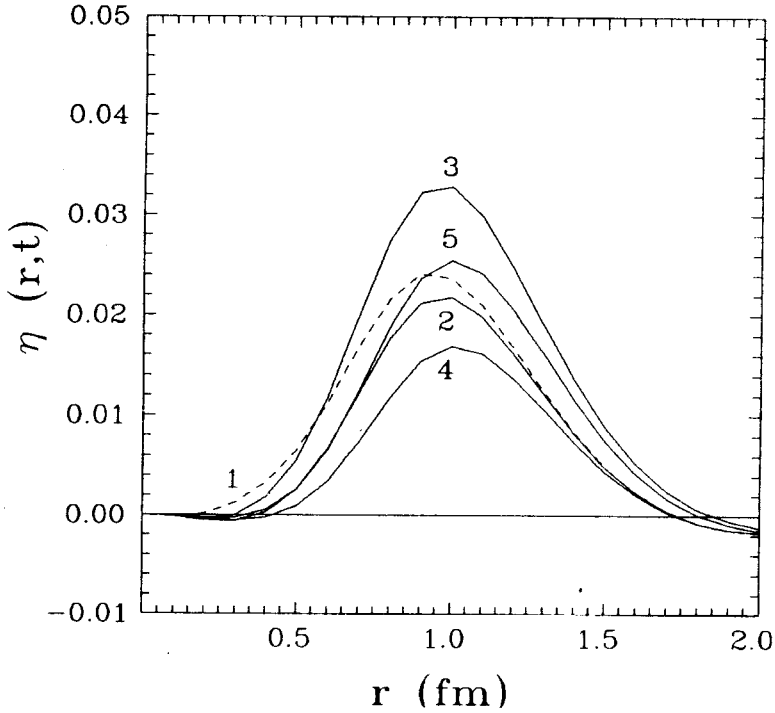


Fig.5. The dashed line 1 is the calculation for point particles. 2 is the inclusion of MEC (S+M), 3 is the inclusion of MEC with allowance for retardation effects (S+M+R) and $\Lambda_\pi = 1.25$ GeV. Calculations 4,5 are the same as 2, 3, but for $\Lambda_\pi = 0.85$ GeV. The calculations were made with the vertex form factor (14) and $t = 30 \text{ fm}^{-2}$

and meson currents, curves 2 and 4, we see, that retardation effects give a very considerable contribution at $t = 30 \text{ fm}^{-2}$. Here, the considered set of meson exchange currents dominates in the range of about 1 fm, which is not in contradiction with the previous result of ref.[7].

4. Conclusion

The investigation of the electrodisintegration of the deuteron near threshold with allowance for retardation effects in MEC allows us to make the following conclusions.

1. The inclusion of retardation effects leads to noticeable discrepancies with experimental data at large transfer momenta ($t > 10 \text{ fm}^{-2}$).
2. The calculations are very sensitive to the value of cut-off parameters and strongly depend on the vertex form factors.
3. The meson exchange currents dominate when the relative distance between two nucleons is of about 1–1.5 fm, when $t < 30 \text{ fm}^{-2}$.
4. Generally speaking, the calculations of the differential cross section with allowance for retardation effects at large transfer momenta force us to take account of other degrees of freedom.

References

1. Hockert J., Riska D.O., Gari M., Huffman A. — Nucl.Phys., 1973, A217, p.14.
2. Lock J.A., Foldy L.L. — Annals of Physics, 1975, 93, p.276.
3. Fabian W., Arenhovel H. — Nucl.Phys., 1976, A258, p.461.
4. Sommer B. — Nucl. Phys., 1978, A308, p.263.
5. Leidemann W., Arenhovel H. — Nucl. Phys., 1983, A393, p.385.
6. Mathiot J.F. — Nucl.Phys., 1984, A412, p.201.
7. Mathiot J.F. — Phys. Lett., 1987, 187, p.235.
8. Burov V.V., Dostovalov V.N., Sus'kov S.Eh. — Czechoslovak Journal of Physics, 1991, 41, p.1139.
9. Gari M., Hyuga H. — Z.Phys. A-Atoms and Nuclei, 1976, 277, p.291.
10. Gari M., Kaulfuss U. — Phys.Lett., 1984, 136B, p.139.
11. Bernheim M. et al. — Phys. Rev. Lett., 1981, 46, p.402.
12. Auffret S. et al. — Phys. Rev. Lett., 1985, 55, p.1362.

Received on October 5, 1992.